Supporting Information:
Biogenic and Anthropogenic sources of Arctic Aerosols

Ingeborg E. Nielsen[1,2], Henrik Skov[1,2,5], Andreas Massling[1,2], Axel C. Eriksson[3,4], Manuel Dall'Osto[6], Heikki Junninen[7,10], Nina Sarnela[7], Robert Lange[1,2], Sonya Collier[8], Qi Zhang[8], Christopher D. Cappa[9] and Jacob K. Nøjgaard[1,2]*

[1]Department of Environmental Science, Aarhus University, Roskilde, 4000, Roskilde, Denmark
[2]Arctic Research Centre, Aarhus University, Aarhus, 8000, Aarhus, Denmark
[3]Division of Ergonomics and Aerosol Technology, Lund University, Box 118, SE-22100, Lund, Sweden
[4]Division of Nuclear Physics, Lund University, Lund, Box 118, SE-22100, Lund, Sweden
[5]Institute of Chemical Engineering and Biotechnology and Environmental Technology, University of Southern Denmark, 5230, Odense, Denmark
[6]Institute of Marine Sciences, CSIC, Passeig Marítim de la Barceloneta, 37-49. E-08003, Barcelona, Spain
[7]Institute for Atmospheric and Earth System Research / Physics, Faculty of Science, University of Helsinki, 00140 Helsinki, Finland
[8]Department of Environmental Toxicology, University of California, Davis, CA 95616, USA
[9]Department of Civil and Environmental Engineering, University of California, Davis, CA 95616, USA
[10]Institute of Physics, University of Tartu, Ülikooli 18, EE-50090 Tartu, Estonia

Correspondence to: Ingeborg Elbæk Nielsen (ien@envs.au.dk)

1 Site Information

25

30
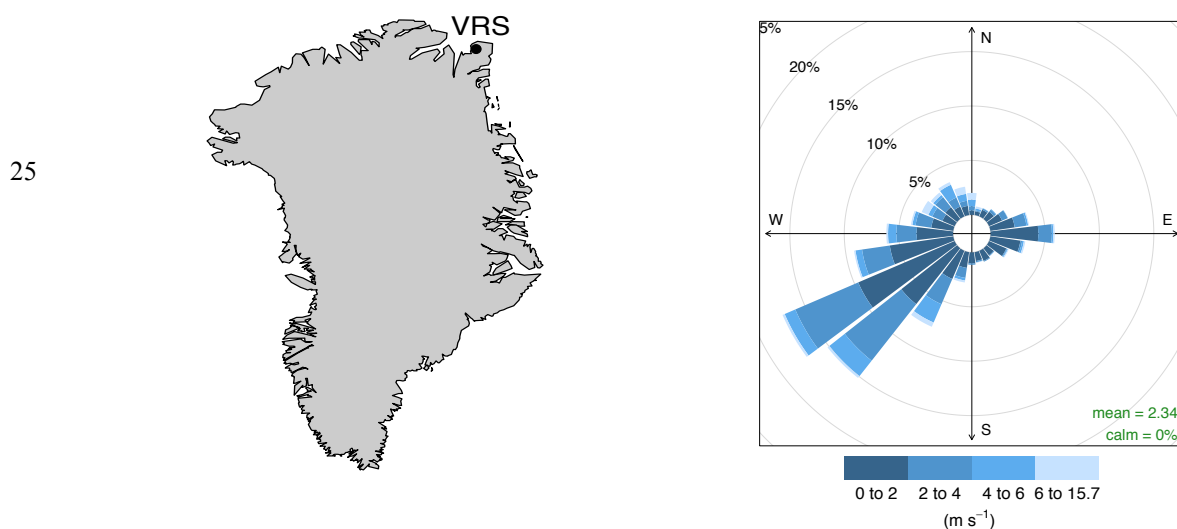
Figure S1. Site information showing a) Map of Greenland including Villum Research Station (VRS), and b) Wind rose with frequency of counts of wind speed [m/s] by wind direction [°] at VRS from 21 February to 23 May 2015.

2 Supplementary Instruments

35 In addition to the soot particle aerosol mass spectrometer (SP-AMS) and multi-angle absorption photometer (MAAP), continuous weekly filter measurements were sampled with a flow rate of 40 L/min on a custom-built filter-pack sampler (FPS) located next to the MAAP. The FPS consists of eight filter packs in series, where one filter pack is used every week, and an extra filter pack used as a field blank. Each filter pack contains three milipore membrane filters – one for collection of particles and the other 40 two for collection of gases (mainly SO_2). The filters were subsequently extracted and analyzed for inorganic aerosols using Ion Chromatography (IC). A more detailed description of the FPS and the IC analysis can be found in Heidam et al. (2004) and Skov et al. (2006). Uncertainty and detection limits are presented in Table S1. Concentrations of elemental (EC) and organic carbon (OC) were determined based on weekly filter samples from a Digitel DHA 80 high-volume sampler (HVS, Digitel/Riemer 45 Messtechnik, Germany). The instrument collected PM_{10} particles on prebaked quartz filters (Advantec, Japan) at a flow rate of 500 L/min, which was subsequently analyzed for EC and OC on a thermal-optical OC/EC instrument from Sunset Laboratory Inc. (Tigard, OR, USA). The analysis followed the EUSAAR-2 protocol (Cavalli et al., 2010) and the detection limits are shown in Table S1.

 Table S1 Detection limit and uncertainty for the FPS and HVS data.

Instruments	Species	Lower Detection Limit	Uncertainty	Reference
FPS, IC	SO_4^{2-}	0.0015 µg S/m^3	20 %	(Massling et al., 2015)
	NH_4^+	0.008 µg/m^3	20 %	(Heidam et al., 2004)
	NO_3^-	0.011 µg/m^3	20 %	(Heidam et al., 2004)
HVS, OC/EC analyzer	EC, OC	0.0045 C µg/m^3	-	(Birch and Cary, 1996)

3 Collection Efficiency and Correlation Plots

Figure S2 The calculated composition dependent collection efficiency (CE) based on Middlebrook et al. (2012).
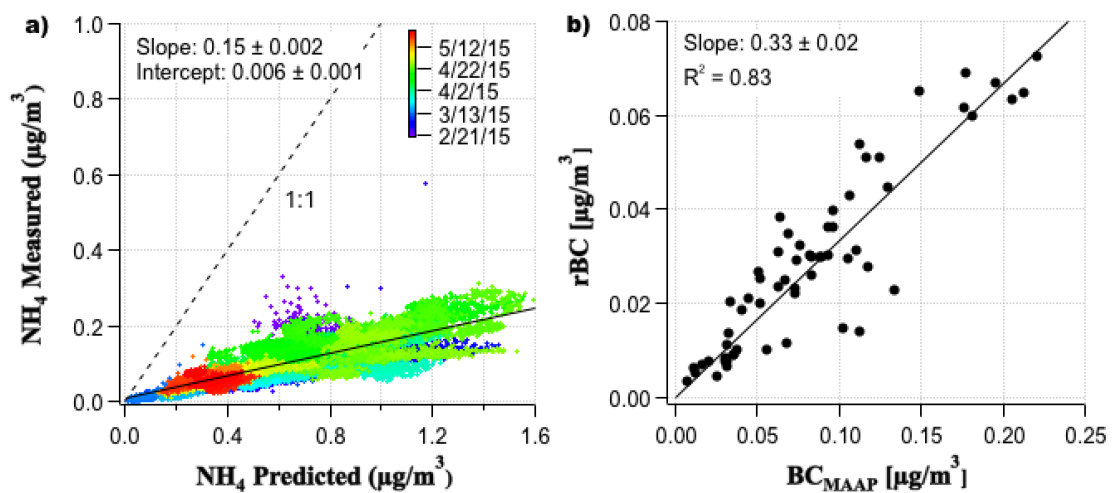
Figure S3 a) Measured versus predicted concentration of NH_4^+ from 21 February to 23 May 2015. A 1:1 line is indicated by the dotted line, and b) Correlation between daily average black carbon from the AMS (rBC) and the MAAP (BC$_{MAAP}$) in µg/m^3 from 21 February to 23 May 2015.
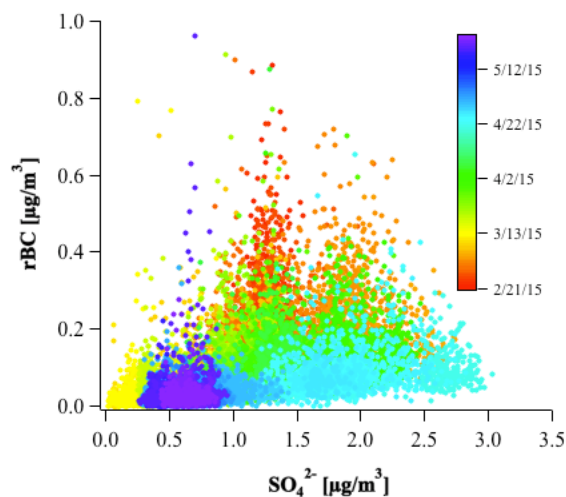
60   **Figure S4** Correlation between rBC and SO_4^{2-} concentrations measured by the SP-AMS from 21 February to 23 May 2015.

4. Validating SP-AMS data

In order to validate the SP-AMS results, the total particle mass concentration (PM$_1$, as estimated by the sum of OA, SO_4^{2-}, NH_4^+, NO_3^-, Cl$^-$ and rBC) was compared with data from the scanning mobility particle

65   sizer (SMPS). The results are presented in Figure S5 as a) a correlation plot between SMPS volume distribution [$\mu m^3/cm^3$] and PM$_1$ [$\mu g/m^3$], b) a correlation plot between SMPS mass concentration assuming an average density of 1.84 g/cm^3 vs. PM$_1$ [$\mu g/m^3$], and c) time series of mass concentration of PM$_1$ from SP-AMS and SMPS (average density of 1.84 g/cm^3). The correlation between PM$_1$ derived from the SP-AMS and volume distribution from the SMPS results in a slope of 2.65 ± 0.03 (orthogonal

70   regression, forced through origin, Figure S5.a). The slope is a simple measure of the average PM$_1$ particle density, which in this case should be 2.65 g/cm^3. However, this density exceeds the expected value, which in theory would be a weighted average of the density for OA, SO_4^2, NH_4^+, NO_3^-, Cl$^-$ and rBC. Since SO_4^{2-} on average makes up almost 70 % of PM$_1$ (Figure 1) it is reasonable to assume an average density of 1.84 g/cm^3, which is the density of sulfuric acid. Applying this density for the SMPS data

75   results in a correlation slope of 1.39 ± 0.01 (orthogonal regression, forced through origin, Figure S5.b). The SP-AMS is hence 39 % higher compared to SMPS results even though the assumed density of 1.84 g/cm^3 for sulfuric acid can be considered a relatively high estimate. Including the densities of organic compounds, NH_4^+ and NO_3^- (around 25 % of PM$_1$) would lower the average PM$_1$ density resulting in a larger difference between the two instruments.
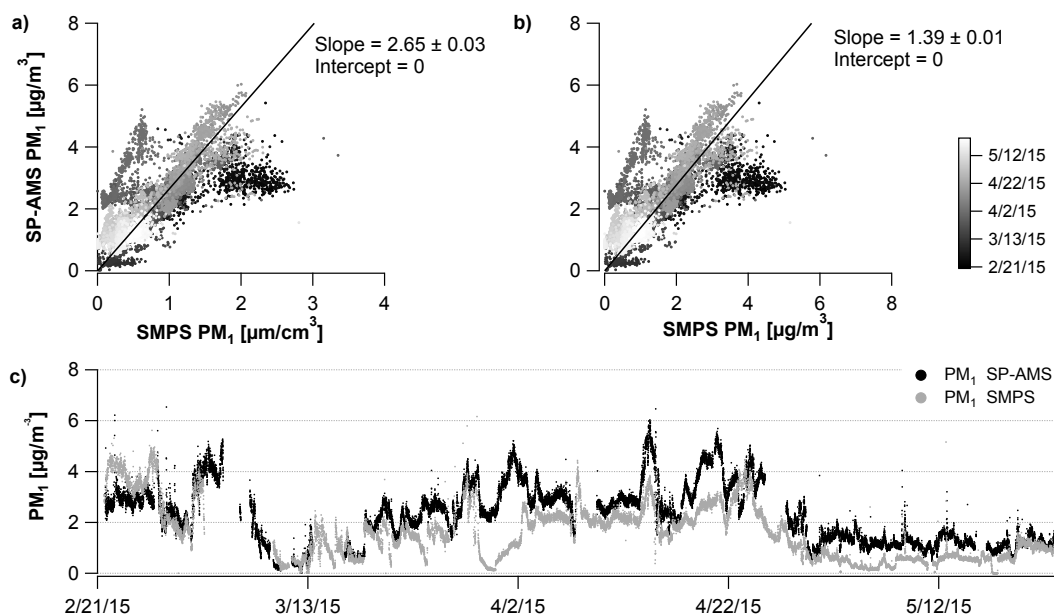
Figure S5 a) Correlation between PM$_1$ mass concentration (sum of OA, SO$_4^{2-}$, NH$_4^+$, NO$_3^-$, Cl$^-$ and rBC) from the SP-AMS and volume distribution from the SMPS, b) correlation between PM$_1$ SP-AMS and SMPS mass concentration applying an average density of 1.84 g/cm^3 for SMPS measurements, c) time series of PM$_1$ concentration from the SP-AMS and SMPS.

The reason for the discrepancies between the two instruments could be due to a range of factors including the different particle size range and location of the two instruments, CE or particle shape. Nguyen et al. (2016) have shown that the dominant size of particles at VRS in winter and spring are in the detection range of the SP-AMS. Therefore, particles exceeding the size of the SP-AMS should not influence the results substantially. The number of particles below the detection range of the SP-AMS (d$_{va}$ < 70 nm) were investigated from the SMPS but were found too minor to have an impact. The instruments are located approximately 300 meters apart in two different measurement huts. However, this shouldn't have an effect on the concentration level since both sites are affected by the same air masses. As previously mentioned the CE was determined based on the time-dependent chemical composition (Middlebrook et al., 2012) with values ranging between 0.7 and 1 (Figure S2). As sulphuric acid is dominating PM$_1$ it is reasonable to assume more liquid particles resulting in CE values close to 1. Hence the time-dependent CE found in this study is a good approximation (Figure S2). The particles are assumed to be spherical, which should be a reasonable assumption for a remote location since the majority of the particles are long range transported and hence highly processed.

Despite the quantification discrepancies between the two instruments the timely pattern is similar and supports the qualitative results of both instruments (Figure S5.c). No explanation could be found for the relatively poor correlation in the beginning of the campaign (21-26 February) and in the end of March (29 March – 2 April), which is why data has not been excluded. It is normal procedure to use an overall instrument uncertainty for the SMPS and SP-AMS of 10 % (for number concentration and higher for volume concentration) (Wiedensohler et al., 2018) and 40 % (Bahreini et al., 2009), respectively. Thus, the differences in concentration range observed between the two instruments are within their uncertainty

range. Furthermore, it is important to keep in mind that the two instruments are measuring aerosol concentration with different methods and complete agreement would not be expected.

Comparison of the SP-AMS results with those of SO_4^{2-}, NO_3^- and NH_4^+ from filter analysis could indicate which instrument measures correctly. However, due to instrumental problems with the FPS this was unfortunately not possible. Instead we have compared the SP-AMS results with the previous five years of weekly data for SO_4^{2-} and NO_3^- from IC, NH_4^+ from an auto-analyzer (AA) and OC from a thermal-optical OC/EC instrument from Sunset Laboratory Inc. (Sunset) (Figure S6). The figure shows that the SP-AMS results corresponds relatively well with the weekly concentration level found the previous five years. The largest discrepancies are found for NO_3^-, which could be explained by the average NO_3^- concentration being close to the detection limit or the fact that the particle size of NO_3^- might exceed the measurement range of the SP-AMS (Fenger et al., 2013). Hence, based on the comparison with the SMPS and knowledge about the general aerosol concentration levels at VRS from previous years we trust the SP-AMS data.
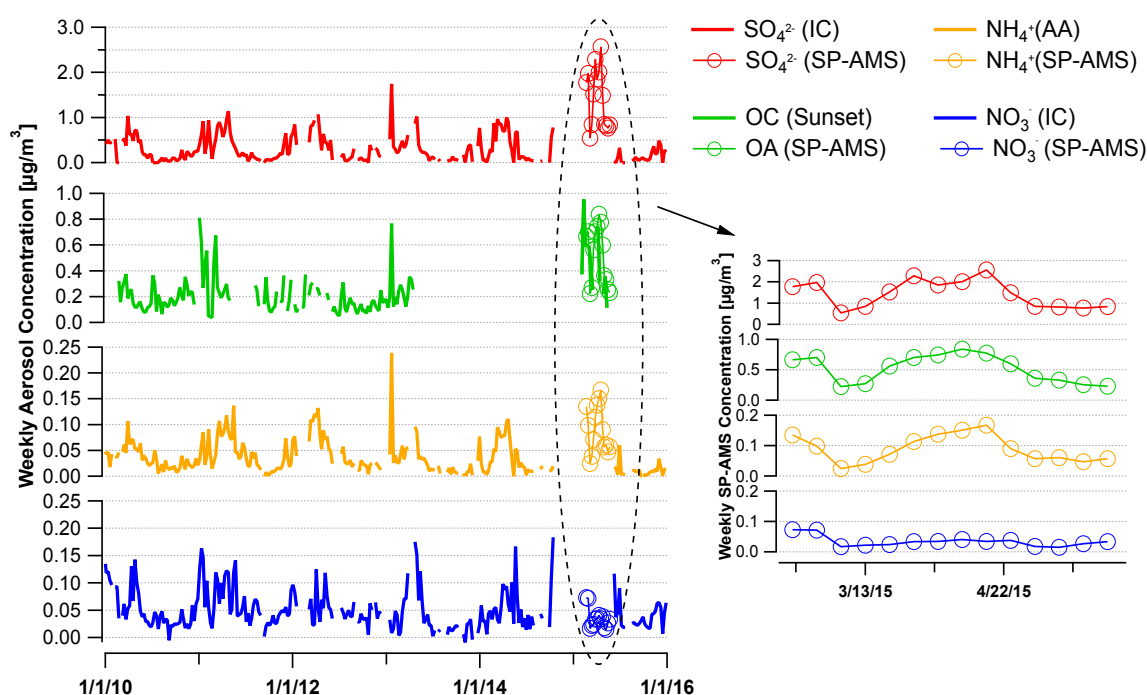
Figure S6 Time series of weekly filter measurements of SO_4^{2-}, NO_3^-, NH_4^+ and OC for 1 January 2010 to 1 January 2016 together with weekly average concentrations from the SP-AMS of SO_4^{2-}, NO_3^-, NH_4^+ and OA for 20 February to 23 May 2015.

5. Key diagnostic plot for the PMF solution

The PMF analysis was conducted on the HR OA mass spectra with 1 to 5 factors. Q/Q$_{expected}$ decreased markedly from 1 to 2 factors, and less from 2 to 3 factors, and 3 to 4 factors. A three-factor solution with a seed value of 0 was chosen and tested for FPEAK values ranging from -1 to 1 in steps of 0.1 Figure S7 presents a summary of the key diagnostics used for evaluating the PMF results. The best solution was

chosen based on Q/Q$_{exp}$ and residuals for the different factors, interpretation of the mass spectra, and correlation with potential tracer species. A FPEAK value of 0 is chosen since *Q/Q$_{exp}$* is at its minimum

130   in the FPEAK range -1 to 0.3 (Figure S7.b).
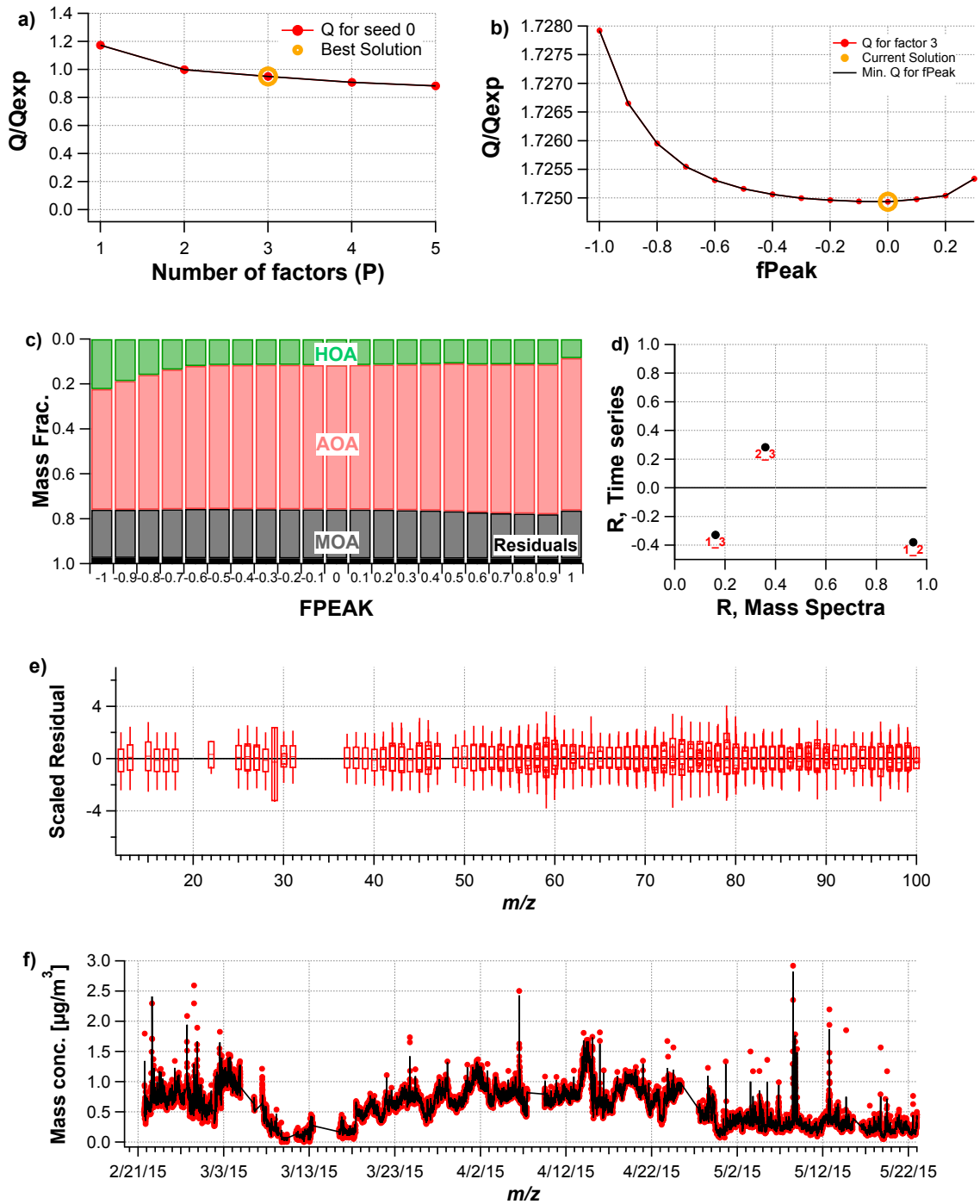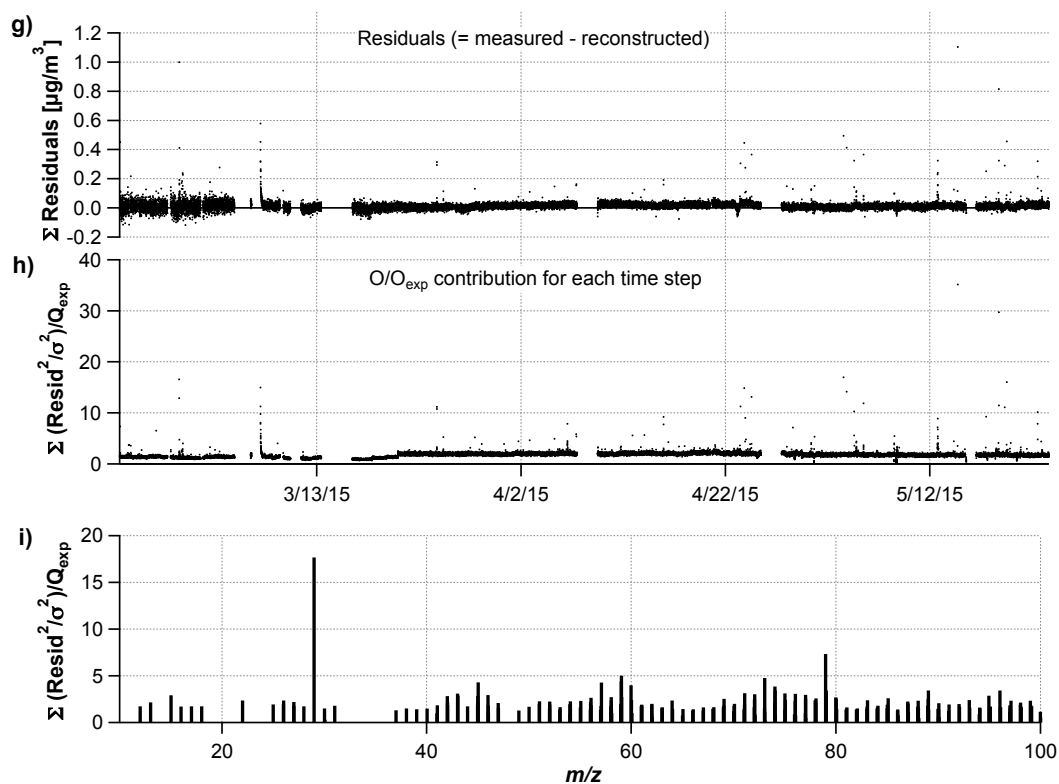
135 **Figure S7** Summary of key diagnostic plots of the PMF results: a) Q/Q_{exp} as a function of the number of factors tested in this study. For the selected three-factor solution with a seed value of 0: b) Q/Q_{exp} as a function of FPEAK, c) the mass fraction of factors vs. FPEAK, d) correlation between factor 1 to 3, e) box and whiskers plot of scaled residual for each m/z, f) times series of the measured and reconstructed organic mass, g) time series of the residuals (measured – reconstructed) of the fit, h) time series of Q/Q_{exp},

140 and i) Q/Q_{exp} vs. m/z.

References

Bahreini, R., Ervens, B., Middlebrook, A. M., Warneke, C., de Gouw, J. A., DeCarlo, P. F., Jimenez, J. L., Brock, C. A., Neuman, J. A., Ryerson, T. B., Stark, H., Atlas, E., Brioude, J., Fried, A., Holloway, J. S., Peischl, J., Richter, D., Walega, J., Weibring, P., Wollny, A. G., and Fehsenfeld, F. C.: Organic aerosol formation in urban and industrial plumes near Houston and Dallas, Texas, J. Geophys. Res.: Atmos., 114, D00F16, https://doi.org/10.1029/2008jd011493, 2009.

Birch, M. E., and Cary, R. A.: Elemental carbon-based method for monitoring occupational exposures to particulate diesel exhaust, Aerosol Sci. Technol., 25, 221-241, https://doi.org/10.1080/02786829608965393, 1996.

Cavalli, F., Viana, M., Yttri, K. E., Genberg, J., and Putaud, J. P.: Toward a standardised thermal-optical protocol for measuring atmospheric organic and elemental carbon: the EUSAAR protocol, Atmos. Meas. Tech., 3, 79-89, https://doi.org/10.5194/amt-3-79-2010, 2010.

Fenger, M., Sørensen, L. L., Kristensen, K., Jensen, B., Nguyen, Q. T., Nøjgaard, J. K., Massling, A., Skov, H., Becker, T., and Glasius, M.: Sources of anions in aerosols in northeast Greenland during late winter, Atmos. Chem. Phys., 13, 1569-1578, https://doi.org/10.5194/acp-13-1569-2013, 2013.

Heidam, N. Z., Christensen, J., Wåhlin, P., and Skov, H.: Arctic atmospheric contaminants in NE Greenland: levels, variations, origins, transport, transformations and trends 1990-2001, Sci. Total Environ., 331, 5-28, https://doi.org/10.1016/j.scitotenv.2004.03.033, 2004.

Massling, A., Nielsen, I. E., Kristensen, D., Christensen, J. H., Sorensen, L. L., Jensen, B., Nguyen, Q. T., Nojgaard, J. K., Glasius, M., and Skov, H.: Atmospheric black carbon and sulfate concentrations in Northeast Greenland, Atmos. Chem. Phys., 15, 9681-9692, https://doi.org/10.5194/acp-15-9681-2015, 2015.

Middlebrook, A. M., Bahreini, R., Jimenez, J. L., and Canagaratna, M. R.: Evaluation of Composition-Dependent Collection Efficiencies for the Aerodyne Aerosol Mass Spectrometer using Field Data, Aerosol Sci. Technol., 46, 258-271, https://doi.org/10.1080/02786826.2011.620041, 2012.

Nguyen, Q. T., Glasius, M., Sørensen, L. L., Jensen, B., Skov, H., Birmili, W., Wiedensohler, A., Kristensson, A., Nøjgaard, J. K., and Massling, A.: Seasonal variation of atmospheric particle number concentrations, new particle formation and atmospheric oxidation capacity at the high Arctic site Villum Research Station, Station Nord, Atmos. Chem. Phys., 16, 11319-11336, https://doi.org/10.5194/acp-16-11319-2016, 2016.

Skov, H., Wahlin, P., Christensen, J., Heidam, N. Z., and Petersen, D.: Measurements of elements, sulphate and SO2 in Nuuk Greenland, Atmos. Environ., 40, 4775-4781, https://doi.org/10.1016/j.atmosenv.2006.03.057, 2006.

Wiedensohler, A., Wiesner, A., Weinhold, K., Birmili, W., Hermann, M., Merkel, M., Muller, T., Pfeifer, S., Schmidt, A., Tuch, T., Velarde, F., Quincey, P., Seeger, S., and Nowak, A.: Mobility particle size spectrometers: Calibration procedures and measurement uncertainties, Aerosol Sci. Technol., 52, 146-164, https://doi.org/10.1080/02786826.2017.1387229, 2018.